Modelling of timber joints in traditional structures

Jorge BRANCO
PhD student
University of Minho
jbranco@civil.uminho.pt

Paulo CRUZ
Associate Professor
University of Minho
pcruz@civil.uminho.pt

Maurizio PIAZZA
Professor
University of Trento
maurizio.piazza@ing.unitn.it

Humberto VARUM
Assistant Professor
University of Aveiro
hvarum@civil.ua.pt

Summary

Original unstrengthened timber connections and the effects of different strengthening techniques have been evaluated experimentally with tests on full-scale birdsmouth joints. Experimental results show that structural response of traditional timber connections under cyclic loading cannot be represented by common constraint models, like perfect hinges or rigid joints, but should be using semi-rigid and friction based models. A research program has investigated the behaviour of old timber joints and examined strengthening criteria. The main parameters affecting the mechanical behaviour of the connection have been singled out. A synthetic model of cyclic behaviour has been adapted on the basis of experimental results.

Keywords: Cyclic behaviour, traditional timber joints, strengthening, experimental testing

1. Introduction

In the field of timber structures, several studies have covered the problem of modelling the behaviour of new engineered connections. Little attention has been devoted to the joints in old, traditional structures that are very frequent in Europe. In Portugal and Italy, for example, timber roof structures, in particular, are part of the constructional tradition, also in earthquake prone areas. From this consideration, the need arises for developing behavioural models of these joints, to be used for the investigation of structural dynamic response [1]. When structural analyses have to be carried out for evaluating the possible need and effect of strengthening, timber are generally impaired by the inadequacy of commercial finite element software in modelling the partial restraint to rotation and the limited moment transmitting capabilities of their connections. The lack of practical, but realistic, models for the joints in old traditional timber structures generally leads to very conservative retrofits and upgrades to satisfy new safety and serviceability requirements. Traditional timber joints, even without any strengthening device, usually have a significant moment capacity. Common constraint models, like hinges or full restraint connections, indeed, cannot satisfactorily describe the real behaviour of these joints. The joint behaviour may be classified as semi-rigid and, being based on friction, is influenced by the time-varying level of compression between the joined members. Joints strengthening can be done in a number of possible ways: from simple replacement or addition of fasteners, to the use of metal plates, glued composites or even full injection with fluid adhesives. Each solution has unique consequences in terms of the joint final strength, stiffness and ductility. The work presented here has been developed within a general research program devoted to the definition of synthetic models for the static and dynamic behaviour description for common timber connections in traditional, old and non-engineered constructions. The study addresses plain timber connections, as well as, connections that are strengthened by steel elements. These devices are extensively used in structural upgrading operations, in order to develop a reliable response in the case of cyclic loading.

2. Model behaviour of semi-rigid timber connections

In recent years, considerable research efforts have been devoted to characterise the semi-rigid connections behaviour, particularly for steel and composite structures. For the case of steel

structures, the case of partial flexibility has been early recognized in design codes, with appropriate values to be obtained either by predictive models or from direct experimentation. Semi-rigid modelling of steel connections in seismic design acknowledges and exploits the dissipation capabilities of their hysteretic behaviour. As recognised by Eurocode 8 [2], a similar approach is appropriate also for traditional timber elements and structures. In the case of existing structures to be rehabilitated or eventually upgraded, according to new requirements, a realistic interpretation of the global structural behaviour is a primary need. In some typical structural configurations of timber constructions, the commonly used hinge models are inadequate; because in real structures, where joints have moment resisting capability, the equilibrium conditions may not be reached analytically. The semi-rigid modelling of timber connections, using nonlinear moment-rotation laws and hysteretic rules, intends to represent the seismic behaviour of timber structures with a comparable level of detail for all the structural components. With these models, the seismic design acknowledges and exploits the dissipation capabilities of their hysteretic behaviour. A numerical model for these connections must, then, be sufficiently accurate to describe properly the semi-rigid behaviour, and sufficiently simple, both conceptually and computationally, to allow use in common practice. Different hysteretic models for timber structures have been developed (Figure 1). Kivell *et al*. [3] derived a hysteretic model for moment resisting nailed timber joints. Dolan [4] and Stewart [5] each developed hysteretic models to describe the cyclic behaviour of timber frame walls with nailed connections between the framing and the sheathing. Ceccotti and Vignoli [6] modelled the pinching hysteretic for moment resisting semi-rigid timber joints made from glulam and drift pins. Although quite different in detail, all these models clearly describe the degrading stiffness for repeated load cycles caused by the plastic deformations of the wood surrounding the fastener. For deformations larger than those that have occurred already in the joint, all the models follow the envelope or skeleton curve of the connection describing its behaviour under static loading.

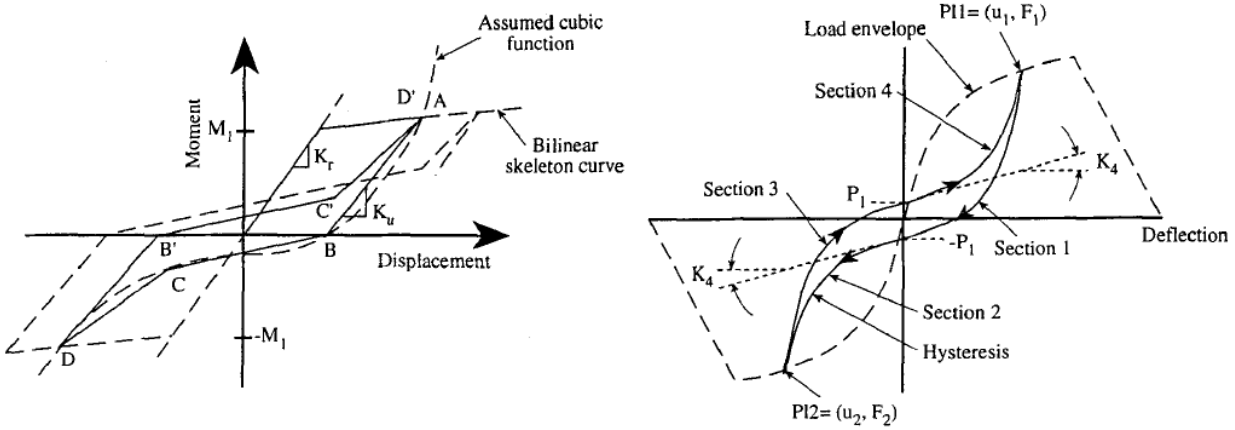

(a) Kivell *et al.* [3] (b) Dolan [4]

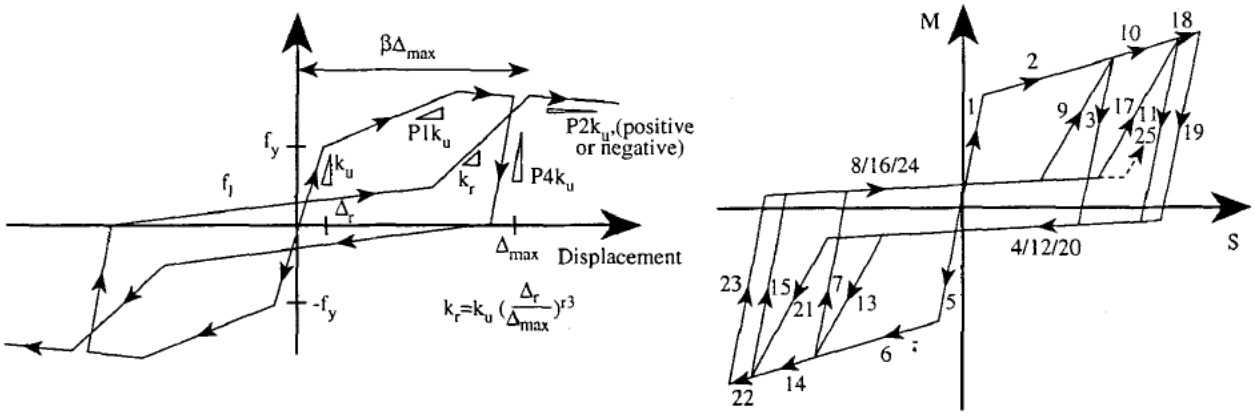

(c) Stewart [5] (d) Ceccotti and Vignoli [6]

Fig. 1 Hysteretic models for timber structures

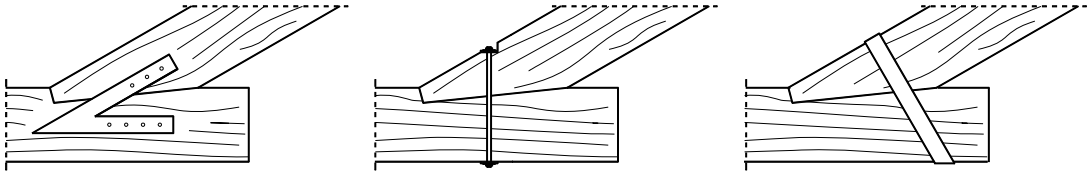

(a) Stirrup (S) *(b) Bolt (B)* *(c) Binding Strip (BS)*

Fig. 4 Traditional strengthening techniques evaluated

Tests on assembled connections were preceded by accurate material characterization, in terms of the mechanical properties of the timber elements used for all full-scale models [9]. Table 1 summarises the test campaign conducted on birdsmouth joints (monotonic and cyclic tests).

Table 1 Tests on birdsmouth joints

Specimen	Type of connection	Loading method	Rafter compression stress level (MPa)
A1, A2, A3	Unstrengthened	Monotonic +	1.4 and 2.5
A4, A5, A6	Unstrengthened	Monotonic -	1.4 and 2.5
A7, A8, A9	Unstrengthened	Cyclic	1.4 and 2.5
S1, S2, S3	Stirrup	Monotonic +	1.4
S4, S5, S6	Stirrup	Monotonic -	1.4
S7, S8, S9	Stirrup	Cyclic	1.4
B1, B2, B3	Bolt	Monotonic +	1.4
B4, B5, B6	Bolt	Monotonic -	1.4
B7, B8, B9	Bolt	Cyclic	1.4
BS1, BS2, BS3	Binding Strip	Monotonic +	1.4
BS4, BS5, BS6	Binding Strip	Monotonic -	1.4
BS7, BS8, BS9	Binding Strip	Cyclic	1.4

The compression stress levels in the rafter adopted: 1.4 MPa and 2.5 MPa, represents, for common Portuguese timber roof structures and according to National standard [10], the dead load applied and the stresses derived from the serviceability limit state, respectively [11].

3.1 Monotonic tests

Test data of original connections have been gathered with the purpose of characterizing their behaviour, as well as, to allow the calibration of numerical models. The tested specimens could not cover all the possible ranges and combination of parameters (as geometry, compression level in the rafter, loading test velocity, etc.) that are of practical interest. The experimental analysis can be extended by numerical models in the next research step. Beyond this, experimentation gave an insight of the joint behaviour for the calibration of the models. It was particularly important to observe the post-elastic behaviour and the failure mode of the connections for each situation analysed. Monotonic tests, meant to inquire the properties of the connection in terms of initial strength, stiffness, and post-elastic deformability. The monotonic tests were carried out both on unstrengthened joints and on joints strengthened with basic types of metal connectors.

The first set of connections tested was composed by three unstrengthened joints (A1, A2 and A3). A permanent compression force of 25 kN (corresponding to 1.4 MPa compression stress) was applied to the rafter throughout the vertical jack, and the second jack imposed a monotonic transversal force (Figure 3). The test results illustrate perfect elasto-plastic behaviour for the three curves (Figure 5). The behaviour is perfectly elastic until the elastic limit displacement (≈8 mm), after which became non-linear but only within a small range. Subsequently, a quasi-perfect plastic behaviour appears. This pseudo-plastic phase, starting at a 10 mm displacement, remains practically constant until the maximum displacement (around 50 mm), presenting a small decrease of the resistance after 25 mm displacement.

3.2 Cyclic tests

In these tests a reduced number of cycles, with increasing amplitude, were imposed. In particular, the test program included one complete cycle with the amplitude [0.25 d_e^+; 0.25 d_e^-]; one cycle in the range [0.50 d_e^+; 0.50 d_e^-]; three cycles in the range [0.75 d_e^+; 0.75 d_e^-]; three cycles in the range [(1+n) d_e^+; (1+n) d_e^-] with n = 0, 1, 2, …. until the failure of the joint. This sequence is in accordance with the proposal in the recommendations of the EN 12512: 2001 [12] (Figure 8). The values used for the elastic limit displacements, for both positive (d_e^+) and negative (d_e^-) directions, came directly from the results previously achieved in the monotonic tests.

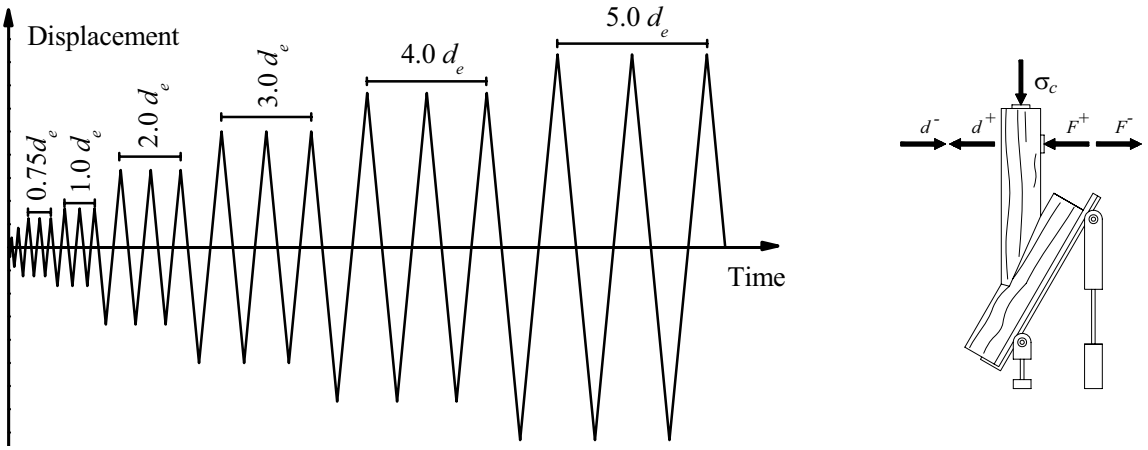

Fig. 8 Cyclic loading procedure adopted

Cyclic tests have been performed on various series of samples of plain timber connections, as well as, connections strengthened by the techniques presented above in Figure 4.

The first observation taken from the cyclic tests on unstrengthened connections is the different response for each direction of loading. Significant energy dissipation occurs only in the negative direction caused by the sliding of the rafter when pulled into this direction. Increasing the compression stress level at the rafter, the force-displacement curves presents an increment in the maximum strength (Figure 9). The energy dissipation grows with the compression stress level in the rafter (2.5% to 3.96% in terms of hysteretic equivalent viscous damping ratio, V_{eq}).

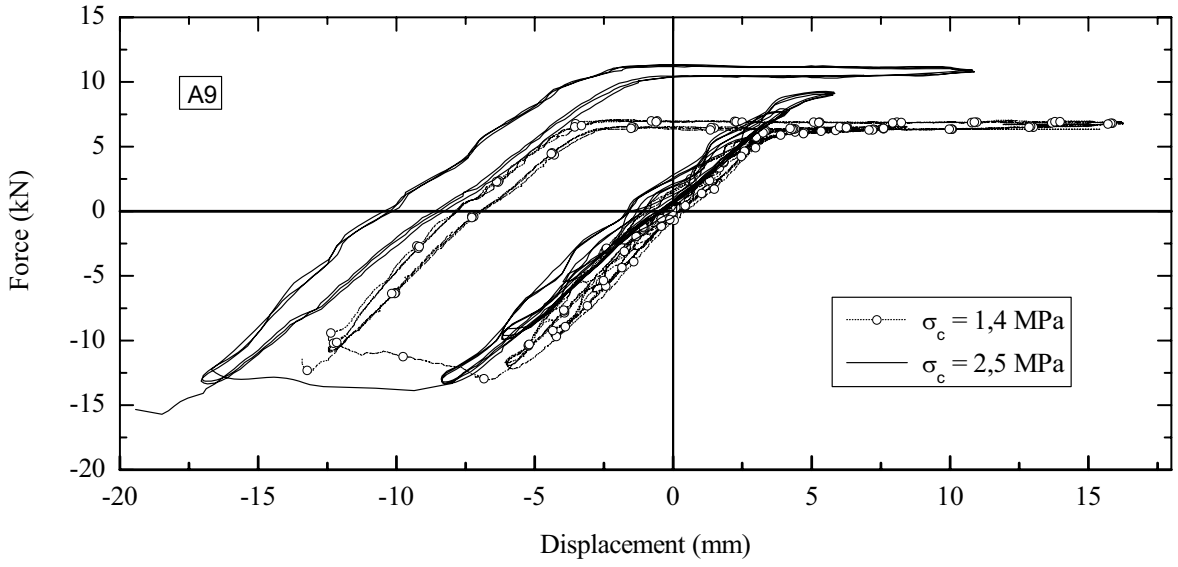

Fig. 9 Influence of the rafter compression stress level in the cyclic response

Observing the cyclic response of strengthened connections and comparing with the original

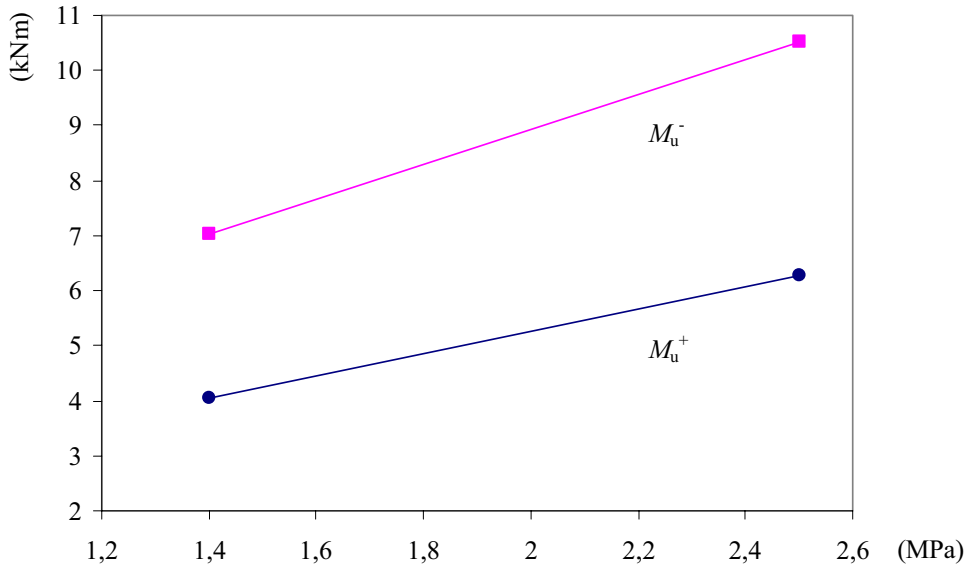

Fig. 11 Ultimate moment M_u versus compression stress level in the rafter (σ_c)

4.2 Modelling of the monotonic tests

The first step in developing a synthetic law of behaviour for the joint considered is to identify a law for first loading, i.e. for the "basic curve", in the cases of positive and negative rotation. As mentioned above, two different approaches are possible, depending on the degree of approximation required. For structures under static monotonic loading, this first loading function describes completely the joint behaviour. An accurate matching of the experimental curve and the model may be feasible by higher order curves, while some simplifications may be advisable in the mathematical description, and mainly in the application, of a cyclic model.

When considering the bilinear approximation, which may be particularly suitable to dynamic analyses from the computational point of view, the first, elastic branch is characterized by a slope k_1^+ or k_1^- and the second branch by k_u^+ or k_u^-, for positive or negative rotations, respectively. The transition point has coordinates (M_y^+, M_y^+/ k_1^+) or (M_y^-, M_y^-/ k_1^-).

The EN 12512:2001 [12] procedure suggests two different methods for the definition of the bilinear approach. The method to use depends on the development of the experimental curve, namely: a) when a clear distinction exists between the elastic and plastic branches; and, b) when is difficult to separate the elastic branch from the plastic one (Figure 12).

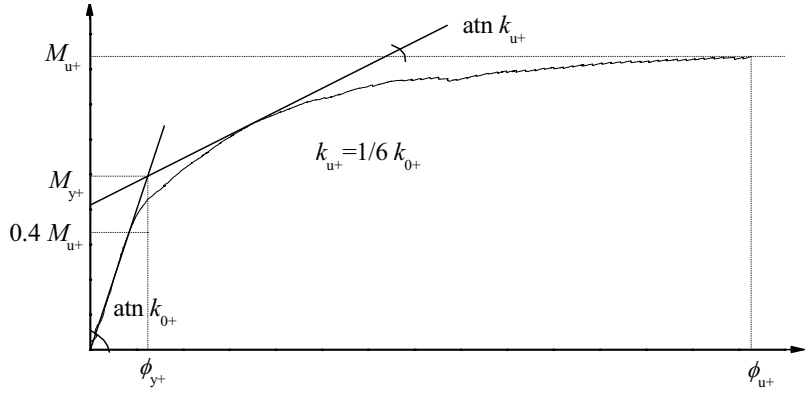

Fig. 12 Method proposed by EN 12512:2001 for the bi-linear approach, when is difficult to separate the elastic branch from the plastic one

There is a wide variety of available hysteretical models in general structural dynamics literature. Together with those that have been proposed for timber joints and structural systems, there seems to be no shortage of hysteretic models that can be used in dynamic analysis of timber structures, and particularly for the traditional timber connections. The main challenges, then, are: 1) selecting the appropriate hysteretic model that should be incorporated in the global structural model and, 2) developing system identification procedures [7].

3. Experimental tests campaign of full-scale timber connections

The experimental research was carried out at the Laboratory of Structures of the University of Minho (Portugal), and includes monotonic and cyclic tests of full-scale birdsmouth joints skew angle of 30º [8].

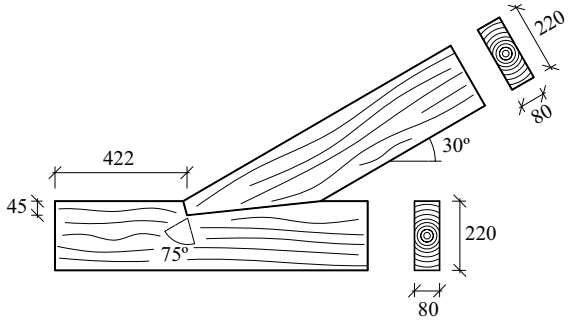

Fig. 2 Connections geometry (dimensions in millimeters)

For all the specimens, the elements have a cross section of 80 x 220 mm^2, the notch depth is 45 mm and the notch length is 422 mm, as represented in Figure 2.

Tests were performed under displacement control. The first step of the loading procedures in both the monotonic and cyclic tests was the application of an axial compression force on the rafter. The axial force, simulating the effect of the self-weight and dead load presented in the structure, was kept constant during the test. In the subsequent loading steps, a transversal force, F, acts perpendicular to the rafter axis.

When the skew angle increases, it is defined as the positive direction and when the skew angle decreases, it is defined as the negative direction.

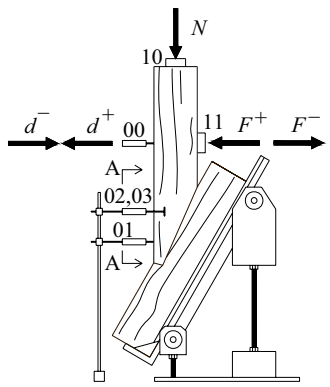

Channels	Transducers
00,01,02,03	LVDTs
10,11	Load cells

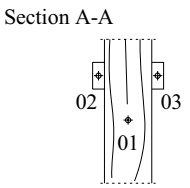

Fig. 3 Testing apparatus and instrumentation layout

Type and location of instrumental channels, including load cells and linear voltage differential transducers (LVDT), are shown in Figure 3.

Firstly, a series of tests on unstrengthened specimens were performed in order to characterize the original behaviour of joints representative of existing timber systems. Subsequently, a set of joints were strengthened with metal devices and tested under monotonic and cyclic loading.

Metal connectors have been applied occasionally in timber joints since very ancient times.

However, this practice became common only in the 19th century, when the development of industrial production methods made bolts, rivets, and other metal elements easily available.

Metal devices were developed and applied basically intending to counteract out-of-plane actions, which could not be resisted by the assemblage itself. Nowadays, strengthening also concerns the behaviour of the friction-based connection in the plane of the structure, and is intended to avoid the detachment of the connected members. The three basic types of intervention considered in this study are modern implementations of traditional strengthening techniques: the stirrups, the internal bolt and the binding strip (Figure 4).

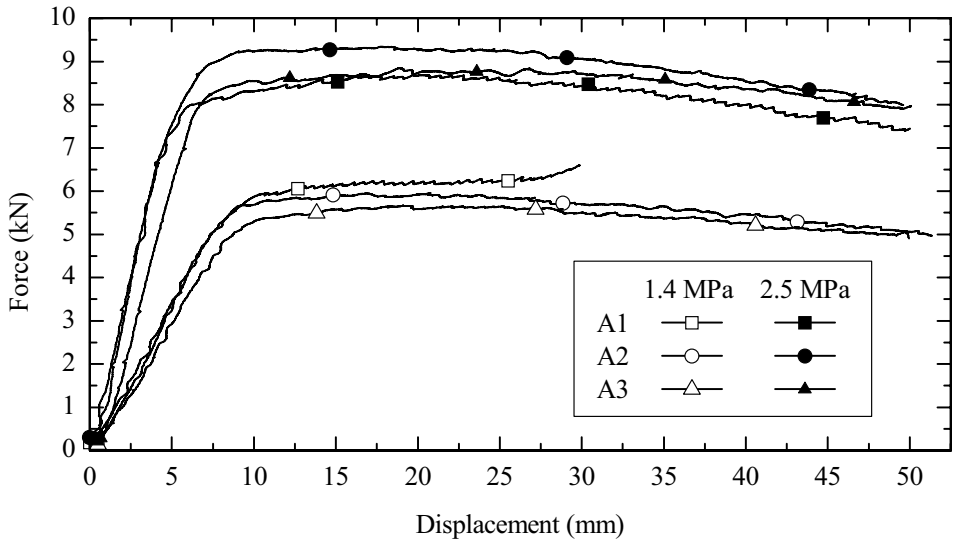

Fig. 5 Force-displacement curves obtained in the positive direction for two rafter compression stress levels

For the opposite direction of loading, a more brittle behaviour was detected when the skew angle decreases. The curves presented in Figure 6 show a behaviour perfectly elastic just at the maximum force, after which a slip, followed by a loss of friction, induces a rapid decrease of the resistance. After the new stable position of the joint is reached, the brittle behaviour is substituted by a pseudo-plastic phase. This ductile behaviour is due to the local compression of wood. Finally, a total loss of friction occurs with the failure of the connection.

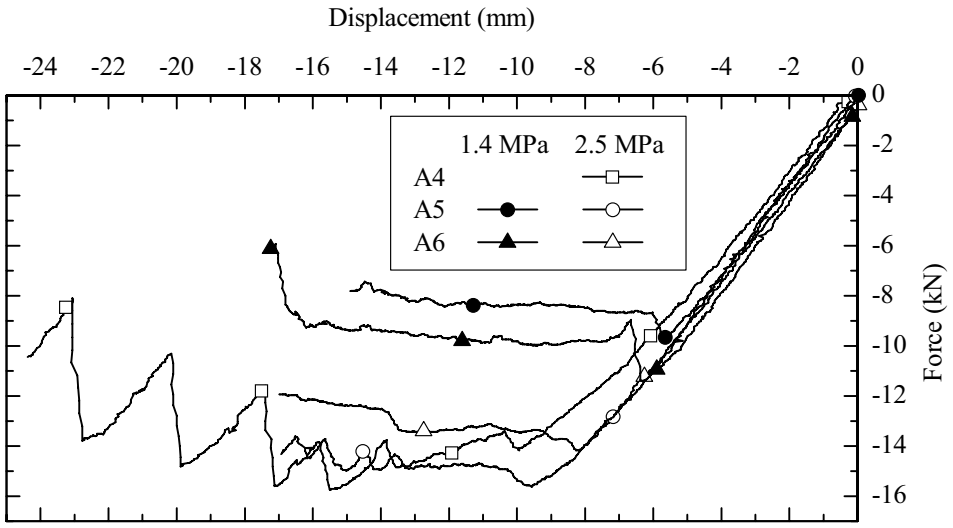

Fig. 6 Force-displacement curves obtained in the negative field for two rafter compression stress levels

Comparing the force-displacement curves obtained from the two different compression stresses in the rafter levels, with the decrease of the skew angle (negative direction), only an increasing in the maximum force and corresponding elastic limit displacement can be observed. Brittle behaviour, after the achievement of the elastic displacement limit, is observed in both cases. The curves, for what concerns the initial stiffness characteristics, remain nearly constant. In the other direction, the positive field, according to the scheme in Figure 3, apart of an increasing in the maximum strength, a higher initial stiffness is also achieved with the increase of the compression stress level in the rafter (Figure 6). However, the behaviour of the curves is similar. Table 2 summarises the main results, average values for the 3 specimens, for the monotonic tests conducted for the two compression stress levels.

Table 2 Influence of the compression stress level in the rafter in the response, for monotonic loading, of the joint

σ_c (MPa)	Direction	d_e (mm)	F_{max} (kN)	Stiffness (kN/mm) x 10^3		
				Regression	F_e / d_e	$F_{e50\%}$ / $d_{e50\%}$
1.4	(+)	8.31	6.72	674	634	647
	(-)	5.76	-10.75	1771	1785	1958
2.5	(+)	5.47	10.84	1569	1389	1408
	(-)	8.13	-15.32	1705	1661	1758

Comparing the test results in terms of force-displacement curves for the unstrengthened and strengthened connections (Figure 7), it is recognized that all the strengthening schemes analysed increase the stiffness, in particular, in the positive direction and the maximum resistance for both directions. The elasto-plastic behaviour with limited ductility evidenced by the unstrengthened connections is substituted by full non linear curves exhibiting high ductility in the strengthened connections. Comparing the strengthening techniques evaluated, the less efficient, in terms of maximum resistance, is the internal bolt, while the elastic stiffness are similar. Connections strengthened with stirrups and binding strip attained the same range of maximum force, however, this last scheme has a lower ductility capacity. In particular, the maximum resistance for the strengthened connections with stirrups and internal bolt is achieved near the end of the test. However, in the strengthened connections with binding strip, when the tests finished, the force value was already decreased. Therefore, between the internal bolt and the binding strip, the first one is more efficient in terms of ductility capacity with the goal to assure a better seismic behaviour of the joints. The effect of the strengthening schemes in the negative directions for the monotonic tests is quite obvious: the maximum resistance and the ductility capacity increase. The benefits in terms of stiffness are not so significant. However, the brittle behaviour exhibited by the original unstrengthened connections disappears in the strengthened specimens. Therefore, the main profit of adding a metal device to the joints is ductility improvement with clear advantages in the seismic response of these structural connections. Only the binding strip showed limitations in terms of maximum displacement.

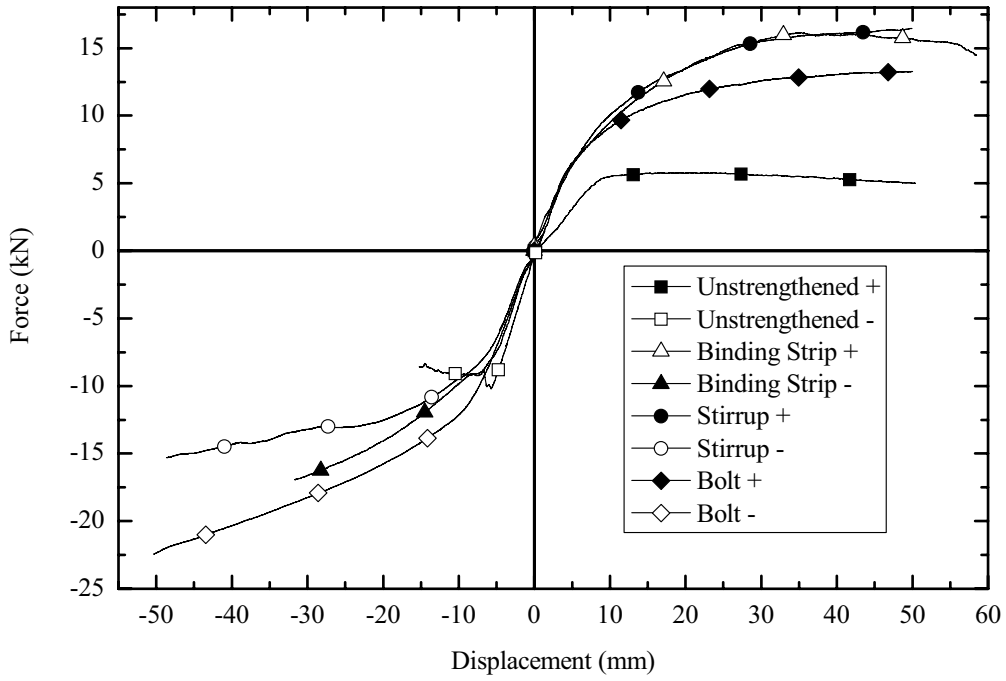

Fig. 7 Force-displacement diagrams for original unstrengthened and strengthened connections under monotonic loading

unstrengthened, under cyclic loading, can be concluded about the positive and negative effects of the strengthening techniques studied. Figure 10 collects the force-displacement diagrams, under cyclic loading, on the strengthened and original unstrengthened joints with a rafter compression stress level of 1.4 MPa.

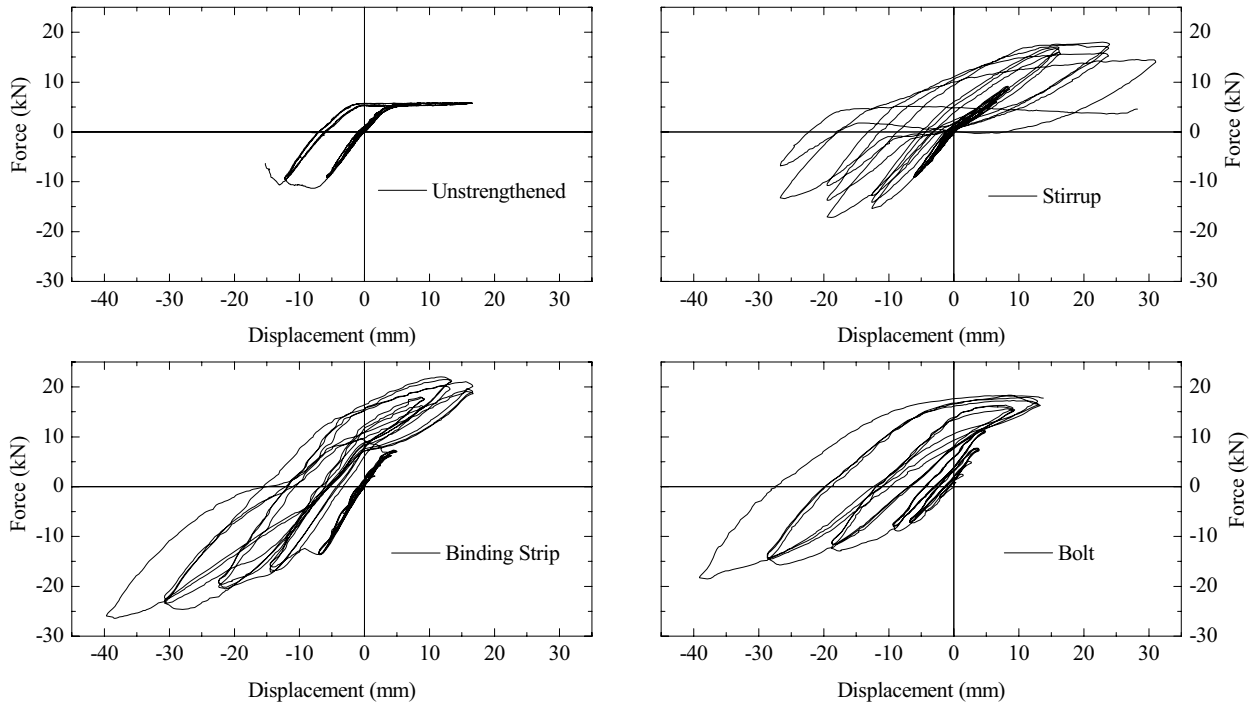

Fig. 10 Force-displacement response for the cyclic loading: original unstrengthened and strengthened connections

The experimental force-displacement diagrams achieved for all connections are asymmetric, both in terms of stiffness and yielding strength. Without strengthening, the joint is not able to prevent the failure caused by load reversals (detachment of the connected elements) and therefore the energy dissipation capacity is very low. All strengthening techniques adopted were efficient in the improvement of the cyclic hysteretic behaviour of the connections. The hysteretic equivalent viscous damping ratio (V_{eq}) evaluated from test results is considerable (Table 3).

Table 3 Main results for the cyclic tests on the original and strengthened joints (average values)

Joint	Dissipated Energy (kJ)	V_{eq} (%)	d_{max}^{+} (mm)	d_{max}^{-} (mm)	F_{max}^{+} (kN)	F_{max}^{-} (kN)
Unstrengthened (σ_c=1.4 MPa)	230	2.45	16.49	-15.83	6.20	-11.57
Unstrengthened (σ_c=2.5 MPa)	380	3.96	9.15	-21.17	9.45	-17.00
Binding Strip (BS)	2874	6.85	18.38	-39.63	23.38	-25.47
Bolt (B)	1877	11.28	13.30	-35.30	15.29	-21.08
Stirrup (S)	1859	14.57	28.68	-21.75	18.09	-15.60

With the increase of cyclic displacement amplitude, the energy is dissipation increases. The number of cycles achieved is particular important taken into account the Eurocode 8 [2] imposition for the behaviour factor. In this standard, it is referred that the dissipative zones shall be able to deform plastically for at least three fully reversed cycles at a static ductility ratio of 4, for ductility class M structures, and at a static ductility ratio of 6, for ductility class H structures, without more than 20% reduction of their resistance.

4. Numerical modelling

4.1 Model parameters

When modelling experimental test results with a synthetic law, a different level of approximation may be adopted for the first loading curve and for the cyclic case [13]. The former describes completely the joint behaviour for structures under monotonic loading. The adoption of a hyperbola permits to describe quite precisely the transition between the elastic and the plastic branches, but a bilinear approximation may also be generally satisfactory.

For a cyclic model to be used in dynamic analyses, some simplifications in the mathematical description are advisable, and a multilinear rule is considered generally adequate [1]. In order to define it, the characteristic intersection points between branches must be derived from the experimental moment-rotation diagrams, M-φ. To this purpose, the following parameters have special importance:

− the initial tangent stiffness, k_0^+ (positive field, increasing skew angle) or k_0^- ;

− the maximum moment and maximum rotation at first loading, determined on the curve of monotonic behaviour, M-ϕ, for positive or for negative rotation (M_u^+, M_u^-, ϕ_u^+, ϕ_u^-);

− the moment and rotation values corresponding to the yielding (transition between the elastic and non-elastic behaviour), M_y^+, M_y^-, ϕ_y^+, ϕ_y^-; Indications for assessing their values and those of the parameters in the following when the non elastic behaviour field can be easily identified or when the mechanical behaviour of the joint exhibits a continuous change of curvature are given in [12];

− the initial secant stiffness, k_1^+ or k_1^-, determined on the straight line connecting the origin and a point of the monotonic curve corresponding to moment values in the range $(0.8\div0.9)M_y^+$, or $(0.8\div0.9)M_y^-$, or in the range $(0.4\div0.5)M_u^+$, or $(0.4\div0.5)M_u^-$, respectively, for the two cases above;

− the coordinates of a point P_1^+ (M_{P1}^+, ϕ_{P1}^+) and of its analogous P_1^- in the negative field, characterising the transition between the elastic and non elastic behaviour; the point P_1^+ may be recovered at a value of the moment $M_{P1}^+ = (0.90\div0.95)\ M_y^+$, or at the value M_y^+ , also in the two cases above;

− the residual stiffness, k_u^+ or k_u^-

These first parameters are common to a monotonic and a cyclic model; the latter requires defining additional values, as follows:

− the secant stiffness at complete unloading, after an excursion in the non elastic field, k_P^+, for the positive, and k_P^-, for the negative quadrant;

− the average residual stiffness passing from the positive to the negative moment, or vice-versa, after an excursion in the non elastic field; it is generally reasonable to assume a single, average value, k_R, instead of the two values k_R^+ and k_R^-

These last parameters may be easily identified in an M-ϕ diagram. In a first approximation and in the absence of specific cyclic testing, they could as well be derived from monotonic ones. Since the values decay, as a function of the extension of non elastic excursion, it has been proposed to derive them from the last cycle of a series of 3 at constant amplitude [14]. Further, it seemed reasonable to consider a series of cycles presenting maximum values of imposed rotation similar to those expected in the numerical application.

One characterising aspect of the friction connections under study is that the ultimate and yield moments, M_u and M_y, are directly related to the level of compression in the rafter. In seismic conditions, significant variations of axial forces in these elements may be expected to occur during the strong motion phase already at medium intensities. Consequently, the relationship between the axial compression level and the limit moments needs to be expressed and included in the synthetic model.

However, using these methods, the synthetic law can present different amounts of energy dissipation when comparing with the experimental curves. Because of that, and since the capability to dissipate energy is crucial in the seismic response, another method was used in this work for the development of the bilinear approximation. The third method applied supports the bilinear approximation which minimize the difference between the energy dissipated in the test results and in the bi-linear curve model (Figure 13).

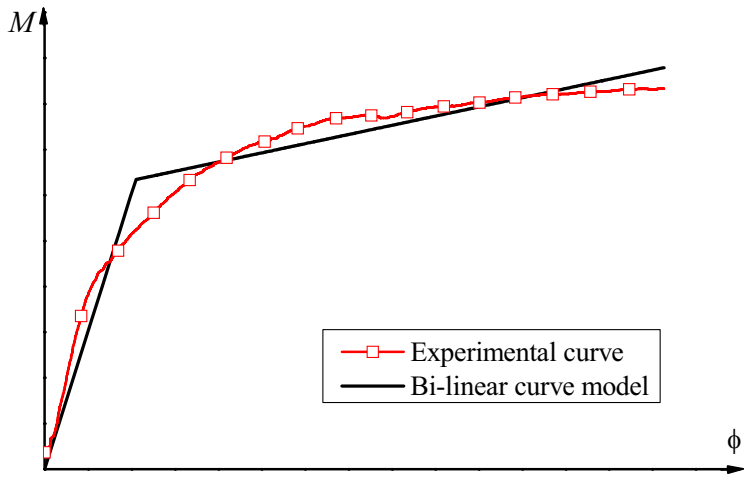

Fig. 13 Bi-linear curve obtained from the minimization of the difference between the energy dissipated

Table 4 presents the comparison between the experimental curve and the synthetic law obtained using the three methods in terms of energy dissipation.

Table 4 Comparison between the energy under the experimental curve and the synthetic law given by different methods (kJ)

Specimen	Experimental	EN 12512 Method (a)	EN 12512 Method (b)	Bi-linear (Same energy)	Tri-linear (Same energy)
B1	496	515	620	494	496
B2	688	705	710	687	684
B3	815	854	630	810	814
B4	885	908	911	885	886
B5	715	728	915	715	716
B6	737	743	844	738	738

With the purpose to obtain a more accurate model, the third method, which gives the same energy dissipation, was adopted in the numerical analysis in this work.

4.3 Modelling of the cyclic tests

It is possible to follow the evolution of the behaviour of a connection under cyclic loading and to define the individual branches composing the corresponding linearised M-ϕ diagram.

The model used in this work is based in the work present by Parisi & Piazza [1]. However, some corrections are introduced and the parameters are adapted based on the test results obtained in the experimental campaign reported in section 3.

Figure 14 highlights the behaviour of the connection at first loading. The first branch, for moments inferior then M_y^+ or M_y^+, is elastic, for positive rotation (1) and negative rotation (3), and characterised, respectively, by a slope k_1^+ or k_1^-. For increasing moment beyond the elastic limit, the connection responds following a second lines branch, with the slope k_U^+ or k_U^-, for positive (2) or negative rotations (4). The transition point has coordinates (M_y^+, M_y^+/ k_1^+) or (M_y^-, M_y^-/ k_1^-), the second branch equation is given by:

$$M^+ = M_y^+ + (\phi - \phi_y^+) \times k_U^+ \quad (1)$$

and

$$M^- = M_y^- + (\phi - \phi_y^-) \times k_U^- \quad (2)$$

for positive and negative rotations, respectively. Moments may undergo variations depending on the level of axial force in the rafter, but, according to experimental evidence, the slope of the plastic branch is not affected and, thus, may be kept constant in the model.

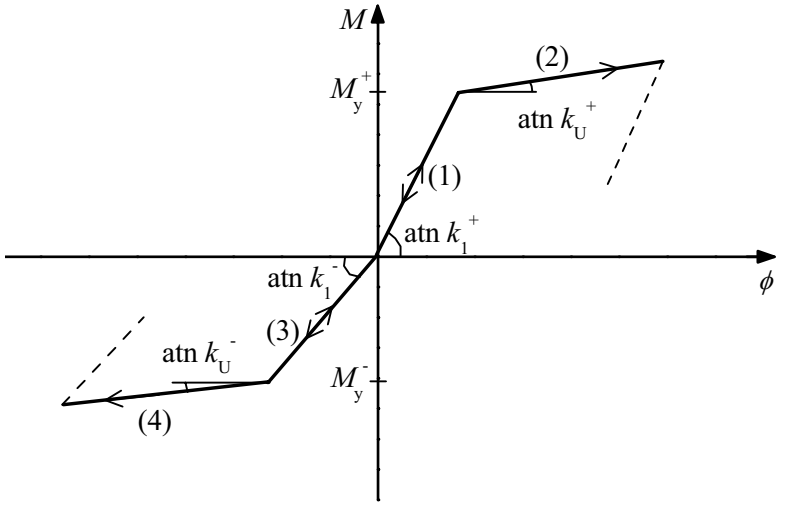

Fig. 14 Model for the cyclic behaviour, part 1 (monotonic loading)

Figure 15 describes the situation of unloading for rotations in the branch (2) or (4) and subsequent unloading. Branches (5) and (6) in the figure are calibrated for unloading.

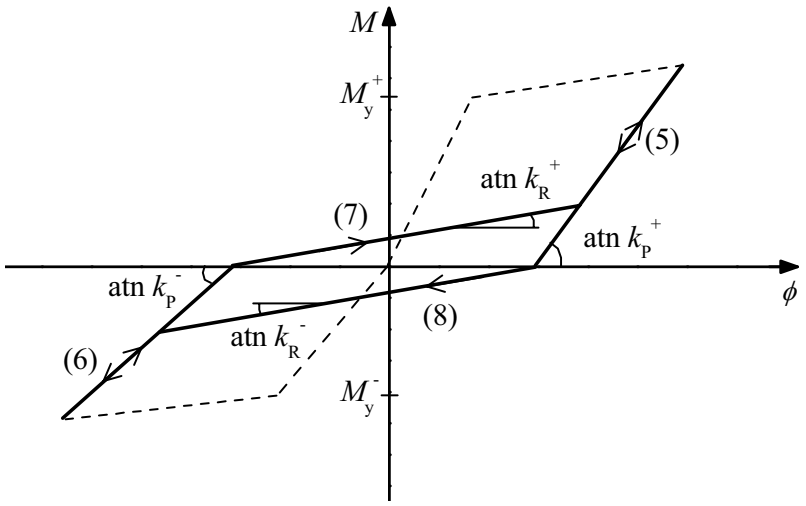

Fig. 15 Model for the cyclic behaviour, part 2 (unloading and reloading)

The unloading stiffness is generally 50 to 80% lower than the elastic one, according to experimental observation [14]. A reduced stiffness, k_P, is adopted for these branches, expressed by the equations

$$M^+ = M_{max}^+ + (\phi - \phi_{max}^+) \times k_P^+ \quad (3)$$

and

$$M = M_{min}^- + (\phi - \phi_{min}^-) \times k_P^- \quad (4)$$

Paths (7) and (8) are followed after complete unloading from the negative and positive quadrant with change of sign of the moment, according to equations

$$M^+ = (\phi_{(6)} - \phi) \times k_R^+ \quad (5)$$

and

$$M = (\phi - \phi_{(5)}) \times k_R^- \quad (6)$$

where $\phi_{(6)}$ and $\phi_{(5)}$ are the rotations on branches (6) and (5) for null moment, respectively.

These low-stiffness branches following unloading are typical of mechanical connections in timber structures. The corresponding residual stiffness, k_R, may be very modest: experimentally, they amounted to 10÷50% of those relevant to unloading branches (5) and (6), depending on the type of strengthening technique.

When unloading occurs from a limited plastic excursion, and because the stiffness k_P is lower than the initial stiffness k_1, branch (5) or (6) may intercept the first loading branch (1) or (3) before the null-moment axis. In this case, that is characterised by an intersection point with all positive (or negative) coordinates, unloading continues along the direction of the first loading branch. A reloading path along segments (5) and (6) will follow branches (2) and (4) upon intersecting them.

In order to simulate pinching correctly, branch (7) continues in the positive quadrant until meeting branch (5) or (1), if previous cycles have reached, or not, respectively, the plastic range in the same quadrant. Similarly, in the negative quadrant branch (8) will join branch (6) or (3). From the intersection onward, stiffness k_P or k_1 is regained. This situation is shown in Figure 16, where subsequent loops activate branches (5) and (6) in loading and unloading.

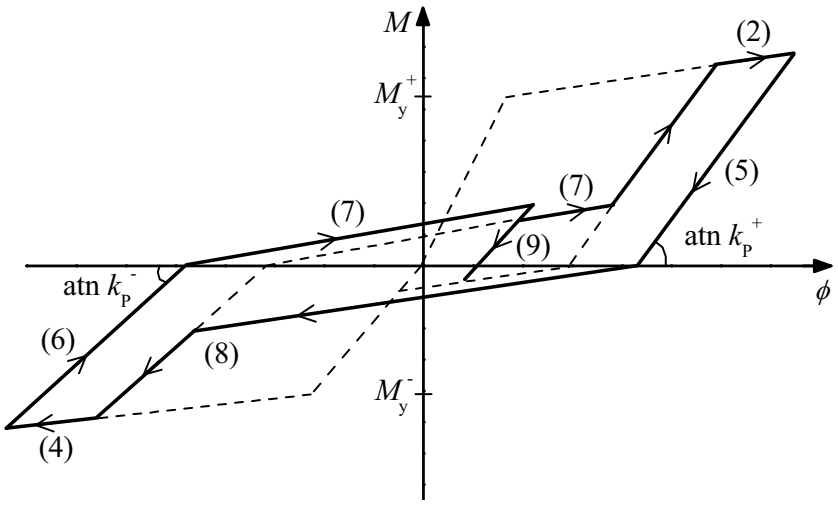

Fig. 16 Model for the cyclic behaviour, part 3 (pinching effect)

After a first loop, linearization may induce, as represented in Figure 17, a slight translation of branches (7) and (8) toward greater moments, in absolute value. This effect is nonsignificant in terms of global response, also considering that, after a small number of initial loops, the connection will remain in the region enclosed by branches (7), (8), (9), and (10), as shown in Figure 17.

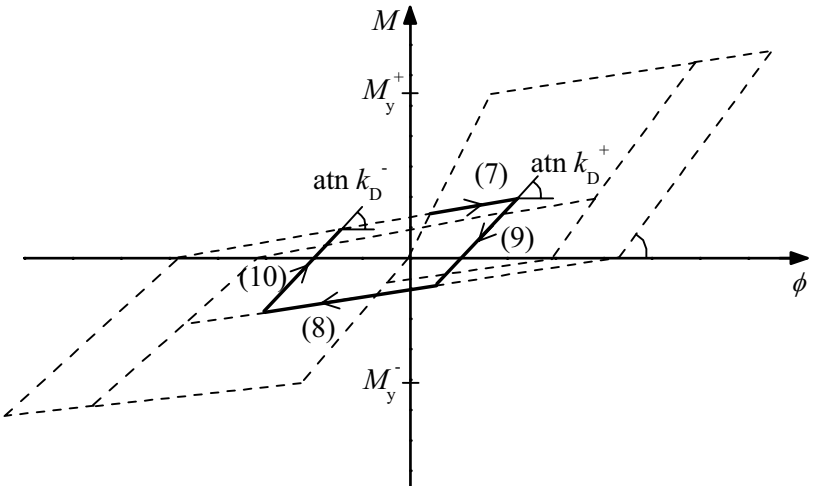

Fig. 17 Model for the cyclic behaviour, part 4 (translation)

Branches (9) and (10) are followed, in loading or unloading, upon moment reversal on the joint from behaviour fields (7) or (8). They represent the situation typical of a joint subjected to low intensity actions after being exposed to rotations of significant value. For these branches, stiffness values included between the initial elastic and the unloading ones are suitable. The same value may be reasonably adopted in both quadrants. The corresponding equations are:

$$M^+ = (\phi - \phi_{7\text{-}9}) \times K_D^+ + M_{7\text{-}9} \quad (7)$$

and

$$M^- = (\phi - \phi_{8\text{-}10}) \times K_D^- + M_{8\text{-}10} \quad (8)$$

where ($\phi_{7\text{-}9}$,$M_{7\text{-}9}$) and ($\phi_{8\text{-}10}$,$M_{8\text{-}10}$) are the coordinates of the points in branches (7) or (8) where the new branch takes over.

From numerical analysis in similar connections [14], the influence of these stiffness values on the global dynamic behaviour is modest. In seismic conditions, however, after the strong motion phase, this area with low residual stiffness may still contribute with a limited energy dissipation. The physical experimentation has shown that, in these cases, it is the friction between coupled surfaces of the elements converging in the node that supplies this energy dissipation contribution in the structural response.

5. Conclusions and final comments

The typical birdsmouth joints, even without any strengthening device, usually have a significant moment-resisting capacity. Therefore, they cannot be represented by common constraint models, like perfect hinges, but should be considered semi-rigid and friction based. The test results show that this capacity is function of the rafter compression stress level. Moreover, it is clear that the width of the rafter, the friction angle, and the skew angle in the connection are also important. The experimental analysis has been of fundamental importance in order to understand the real behaviour, by pointing out some important aspects like force transmission mechanisms, failure modes and guidance for appropriate strengthening solutions. Strengthening, usually performed by insertion of metal devices, is indispensable for ensuring adequate joint response, in particular, for seismic loading, or in other adverse and unpredictable loading conditions. The strengthening of the joints results in a significant increase of the hysteretic equivalent viscous damping ratio (V_{eq}). The energy dissipation became significant. In conclusion, the strengthening solutions studied improve the seismic behaviour of the birdsmouth joints typically presented in traditional timber roofs.

The possibility of modelling these connections numerically, by means of nonlinear moment-rotation laws and hysteretic rules, intends to represent the seismic response of timber structures with a comparable level of detail for all the structural components. The paper presents a model for interpreting the cyclic, semi-rigid behaviour of traditional joints in timber structures, along the guidelines of the European Codes. The model is based in previous works [1] and on the results of experimental results of full-scale birdsmouth joints. Next step of the research program will be the implementation of the hysteretic models in a finite element format.

6. Acknowledgments

The first author gratefully acknowledges the Portuguese Foundation for Science and Technology, for his PhD grant, with the reference SFRH/BD/18515/2004. The research described in this paper was conducted with financial support of the Portuguese Foundation for Science and Technology (contract reference POCI/ECM/56552/2004). This work has been carried out with a partial financial contribution of the Italian Earthquake Engineering Laboratory Network (RELUIS).

7. References

[1] Parisi, M.A. and Piazza, M., "Seismic behaviour and modelling of traditional timber roof structures", Proceedings, *11th European Conference on Earthquake Engineering*, Paris, 1998.

[2] prEN 1998-1:2004, *Eurocode 8: Design of structures for earthquake resistance. Part 1: General Rules, Seismic Actions and Rules for Buildings*, CEN, European Committee for Standardization. Brussels, Belgium.

[3] Kivell, B. T., Moss, P. J. and Carr, A. J., "Hysteretic modelling of moment resisting nailed timber joints", *Bull. New Zeal. Nat. Soc. Earthquake Engineering,* 14(4)(1981) 233-245.

[4] Stewart, W. G., *The seismic design of plywood sheathed shear walls*, Ph.D. thesis, University of Canterbury, Christchurch, New Zealand, 1987.

[5] Dolan, J. D., *The dynamic response of timber shear walls*, Ph.D. thesis, Department of Civil Engineering, University of British Columbia, Vancouver, BC, Canada, 1989.

[6] Ceccotti, A. and Vignoli, A., "Engineered timber structures: An evaluation of their seismic behaviour", in Proceedings, *1990 International Timber Engineering Conference*, Tokyo, Japan, pp. 946-953.

[7] Foliente Greg C., "Modeling and Analysis of Timber Structures Under Seismic Loads: State of the Art", *Earthquake Performance and Safety of Timber Structures*, Ed. By Greg C. Foliente. Forest Products Society, Madison, 1997, ISBN 0935018859, USA, p. 5573.

[8] Branco J., Cruz P. and Varum H., *Experimental Analysis of Birdsmouth Joints,* Report E-11/05. DECivil, University of Minho, 2005, 49 pp.

[9] Branco J., Varum H. and Cruz P., "Structural grades of timber by bending and compression tests", *Advanced Materials Forum III*, Materials Science Forum, Trans Tech Publications Inc., ISBN 0-87849-402-2, Vol. 516, pp. 1163-1167.

[10] RSA 1983, *Regulamento de Segurança e Acções para Estruturas de Edifícios e Pontes,* Dec. – Lei n.º 235/83. Casa da Moeda. 31 May (in Portuguese).

[11] Branco J., Cruz P., Varum H. and Piazza M., *Portuguese traditional timber trusses: static and dynamic behaviour,* Report E-19/05. DECivil, University of Minho, 2005, 50 pp.

[12] EN 12512: 2001, *Timber structures - Test methods – Cyclic testing of joints made with mechanical fasteners*, CEN, 2001, Brussels, Belgium.

[13] Parisi, M.A. and Piazza, M., "Dynamic modelling of friction joints in traditional timber structures", Proceedings, *EURODYN 99 Conference*, Prague, 1999.

[14] Fumanelli, M., *Analisi teorico-sperimentale del comportamento sismico di coperture lignee tradizionali*, Graduation Thesis, Curriculum in Civil Engineering, University of Trento, Italy, 2001 (in Italian).